

# Numerical Comparison between Turbulent Models in Flow past Two Buildings of Different Heights

M. M. Nassief

Associate Professor, Faculty of Engineering, Zagazig University  
(Mofreh\_melad@yahoo.com)

**Abstract-** The states in the flow regime past two circular buildings, tall- short and short- tall in tandem arrangement (TSA and STA of  $H/h=3$ ) are investigated. The effect of building gap ( $L/D=1.5, 2, 2.5$  and  $3$ ), diameter ratios ( $0.5 \leq B \leq 3$ ) and different turbulent models ( $k-\epsilon$ ,  $k-\epsilon$  (RNG) and LES) at Reynolds number ( $200 \leq Re \leq 3000$ ) are taken into consideration. A plane of  $Z/H=0.05$  is taken to get the details of flow in all study cases. The results demonstrate that the  $k-\epsilon$  (RNG) turbulent model is more suitable for these applications than the other turbulent models. Also there are notable changes to the response of the flow as result of variation of buildings separation and the vortex structures at  $Re=3000$  are much stronger as compared to those at  $Re=200$  according to the variation of Strouhal number ( $St$ ) with  $Re$ , also the positive drag coefficient increases as the diameter ratio increases and more higher for the short building (either front or rear) than the tall one. The gap  $L/D=2.5$  is found to be critical for all turbulent models due to abrupt changes in flow characteristics. At some gap values the downstream buildings have higher values of average drag coefficients as compared to upstream one.

**Keywords-** cylindrical buildings; three dimensional; unsteady incompressible flow; tandem arrangements; turbulent models

## I. INTRODUCTION

In the external flow around solid bodies, it is a well-known fact that the presence of other bodies in close proximity may change the fundamental aspects of the flow such as fluid forces and transition thresholds. The effect of the presence of additional bodies in the fluid stream is called flow interference. A particular type of flow interference which is especially severe is the wake interference, and happens when one body is immersed in the wake of another body. Building designers usually refer to codes practice to determine wind loads on buildings. These codes are usually based on measurements in boundary layer wind tunnels. However, several building configurations are not covered by these codes. One such configuration is the pitched – roof building and in the case of bluff bodies, the most commonly applied model to study wake interference is the flow around two different circular buildings placed in tandem arrangements, Mof. (2014). Zaheer et al. (2011) in his review, showed that many researchers made significant contributions in the field of computational wind

engineering in the last few decades. They concluded that the discrepancies in the pressure coefficient variations of TTU building model with wind tunnel testing results are due to the improper simulation in 2-Dim. A.Sohankar (2012), used a range of Reynolds number from 40 to 1000 and a gap spacing of  $4D$  where  $D$  is the cross sectional dimension of cylinders, he applied an incompressible finite volume code with a collected grid arrangement to carry out the flow simulation. He concluded that three major regimes are distinguished according to the normalized gap spacing between cylinders. That is, the single slender –body regime ( $gap < 0.5$ ), the reattach regime ( $gap < 4$ ) and co-shedding or binary vortex regime ( $gap \geq 4$ ) and hysteresis with different vortex patterns is observed in a certain range of the gap spacing and also for the onset of the vortex shedding. I. Ehsan et al. (2013) used a range of  $1 < Re < 200$  and  $1 \leq G \leq 9$  and the fluid viscosity law index lies in the range  $0.5 \leq n \leq 1.8$  which covers shear-thinning Newtonian and shear thickening fluids. They concluded that in comparison to Newtonian fluids, it is found that the onset of leading edge separation occurs at lower Reynolds number for shear thinning fluids and is delayed to large values for shear-thickening fluids. Y.Kada et al. (2013) used a Lattice Boltzman method in two and three dimensions simulations for one and two cylinders with cylinders spacing in the range of  $1.5d$  to  $8d$  at  $Re$  number in the range of 160 to 220. They concluded that for the Reynolds numbers studied, the forces acting on the upstream cylinder were less affected by the 3-Dim.instabilities than in the single cylinder case. Y. Gao et al. (2013) investigated the wake structure behind a circular cylinder- pair of unequal diameters as a function of incident flow angle  $\alpha$  using the particle image velocimetry technique with  $Re$  number ,center to center spacing ratio and diameter ratio are kept constant at 1200 ,1.2, and 2/3 respectively. They concluded that the flow patterns behind the cylinder-pair change from that of a single bluff body to two vortex streets with increasing incident angle over the range of  $0 \leq \alpha \leq 90$ , while the inverse phenomenon is observed when  $90 \leq \alpha \leq 180$ .Kopp G.(2014) Tested Scale models in a boundary layer wind tunnel and examined the effect of building size and array geometry on enveloping curves of area averaged pressure coefficient. He concluded that for tilt angles less than  $10^\circ$  the increase in the pressure coefficient as the tilt angle increases is approximately linear. Renjie et al. (2014) deduced flows past 2 tandem cylinders of different diameters placed in a free-stream velocity and between 2 parallel walls numerically via a Lattice Boltzmann

method. They concluded that for both the unconfined and confined cases vortices are shed from both cylinders in a coupled frequency which is mainly dependent on the front cylinder in contrast with case of an isolated cylinder. Ming et al. (2014) investigated viscous fluid flow past 2 identical circular cylinders in tandem arrangement at  $Re=200$  by considering a large span of spacing ratio ( $0.1 \geq L/D \leq 6$ ) with a fine interval of 0.1 or less. They concluded that the phase difference between the lift fluctuations of the 2 cylinders provides further understanding to the dependence of the wake evaluations behind the twin circular cylinders. Verma (2014) investigated the wind loads experimentally on rigid models of rectangular shape high rise buildings, the models made from Perspex sheet 5mm in thickness and the pressure taps are made on models to measure the pressure distribution. He concluded that negative pressure on opposite faces gets increased considerably when the models are close to each other. Micheal Jesson et al. (2015) deduced experimentally the transient aspects of down burst- like flow, allowing the pressure distributions they create over cube and portal formed structures to be measured. They concluded that the mean turbulence intensity of the radial velocity varies between 3% and 10% depending on which method is used to calculate it. From the above discussion, it can be deduced that much less attention has been given to the studies for flow past two circular buildings of different height and diameter, with different turbulent models. In the present work, the investigation concerns how the three -dimensional unsteady flow with variation of gap, Re, diameter and turbulent model affect the wake region and so the drag forces for two cylindrical buildings; of diameter/height=0.25; in tandem arrangements. The flow states were obtained for ( $200 \leq Re \leq 3000$ ) by means of numerical simulation for different turbulent models.

## II. NUMERICAL TECHNIQUE

The prediction of air – flow characteristics around two cylindrical buildings arranged in tandem requires the application of a computational fluid dynamics (CFD) program. ANAYSES 15.0.7 [15] is a computer package used for predicting the air – flow characteristics. The program is a three - dimensional one, which utilizes the finite –volume approach and a grid of 500000 nodal points, which uses different turbulence models and solves the continuity and momentum equations. In the present work, the boundary conditions stipulate no slip and no penetration. This means that the flow velocity at all the solid surfaces is zero (satisfying the real viscous fluid configuration), as shown in Fig. 1. Also, the approaching velocity profile is uniform and the fluid is Newtonian. The flow is a single-phase, unsteady incompressible. The solution domain consists of constant geometry and the body forces are neglected. Thus, the governing equations can be expressed as follows:

### A. Continuity equation (conservation of mass)

$$\frac{\partial u}{\partial x} + \frac{\partial v}{\partial y} + \frac{\partial w}{\partial z} = 0 \quad (1)$$

### B. Momentum equation

The momentum equation of motion in tensor form for turbulent flow is given by:

$$\frac{\partial u_i}{\partial t} + \frac{\partial}{\partial x} (u_i u_j) = - \frac{1}{\rho} \frac{\partial p}{\partial x_j} + \frac{1}{\rho} \frac{\partial}{\partial x_i} \left\{ (\mu + \mu_t) \left( \frac{\partial u_i}{\partial x_j} + \frac{\partial u_j}{\partial x_i} \right) - \frac{2}{3} \delta_{ij} K \right\} \quad (2)$$

Consideration must be specified as stated above and shown in Fig.1. More details of the solution of the above governing equations based on the turbulence models are given in ANYSES 15.0.7. Also according to Roshko,s (1955) and Sreenivasan et al. [12], the expression that relates vortex frequency shedding (f) behind a longer cylinder ,the diameter of cylinder (D), the kinematic viscosity ( $\nu$ ) and Re is given by: ( $f D/2\nu = 0.212Re - 4.5$ ) and since the Strouhal number (St) is given by:  $St = f D/U_\infty$ , where  $U_\infty$  is the up-stream velocity therefore,  $St = \nu (0.212Re - 4.5)/D U_\infty$ .

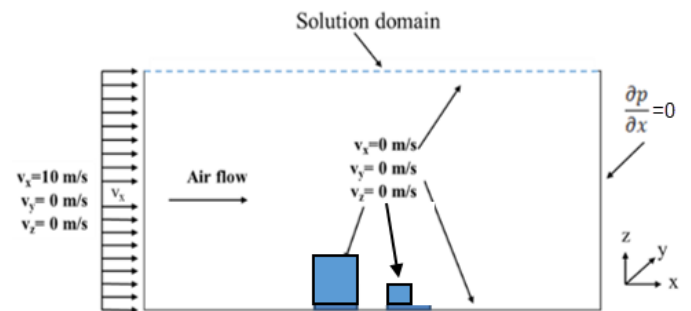


Figure 1. Boundary conditions and solution domain

## III. RESULTS AND DISCUSSION

A number of three-dimensional simulations around two cylindrical buildings were performed to investigate the flow pattern in tandem arrangements, fixing the heights of geometric configuration and varying of both L/D and diameter ratio, the schematic diagram of buildings is shown in Fig.2.

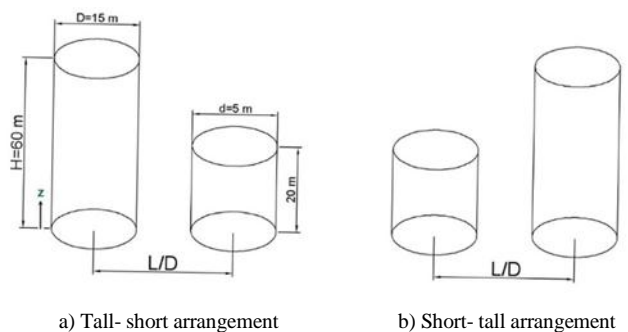


Figure 2. Schematic diagram of the buildings in tandem arrangement

In this section a detailed analysis of different flow patterns, revealed in this study is presented in terms of pressure and drag coefficients, Strouhal number, velocity vectors patterns, and pressure contours.

### A. Validation of Code

For the purpose of the validation of the solution procedure, it is essential that numerical simulations be compared with other results. Fig. 3 compares the pressure coefficient (CP) of the present work (with applying k-ε (RNG) as a turbulent model other than the other turbulent models) with the experimental results of Mofreh [1] for the upstream building.

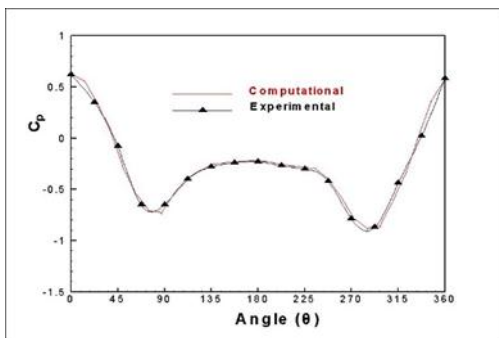


Figure 3. Comparison of experimental results of Mofreh [1] and the present work results

This figure shows a good agreement between the present numerical results and the other results. It can therefore conclude that the CFD code with k-ε (RNG) as a turbulent model can be used to solve the flow field for similar geometries and conditions.

### B. k-ε Results

Figures (4a,b,c and d) show Cp contours of STA and TSA for different gaps (L/D=1.5, 2, 2.5 and 3) and at plane (Z/H=0.05). It is shown in all figures that different vortex shedding regimes can be observed in the flow around this type of arrangement, depending on the center-to-center separation (L/D), also the stagnation point at the front building is clear but it is not clear at the rear one in TSA especially at L/D=1.5, this is because the rear building lies in the wake region of the front tall building but in STA the two stagnation points are clear for the two buildings. For all different L/D values, the vortex shedding regime is symmetric in gap as shown in figures. In this regime, a pair of almost symmetric vortices is formed in the gap between the buildings and the root mean square of the lift on the downstream building is small. If the gap is gradually increased to L/D=3 as shown in figures the vortex shedding regime eventually changes to alternating in gap in which regions of concentrated vortices grow and decrease alternatively on each side of the line that links the centers of the buildings this makes the root mean square of the lift coefficient on the downstream building increases.

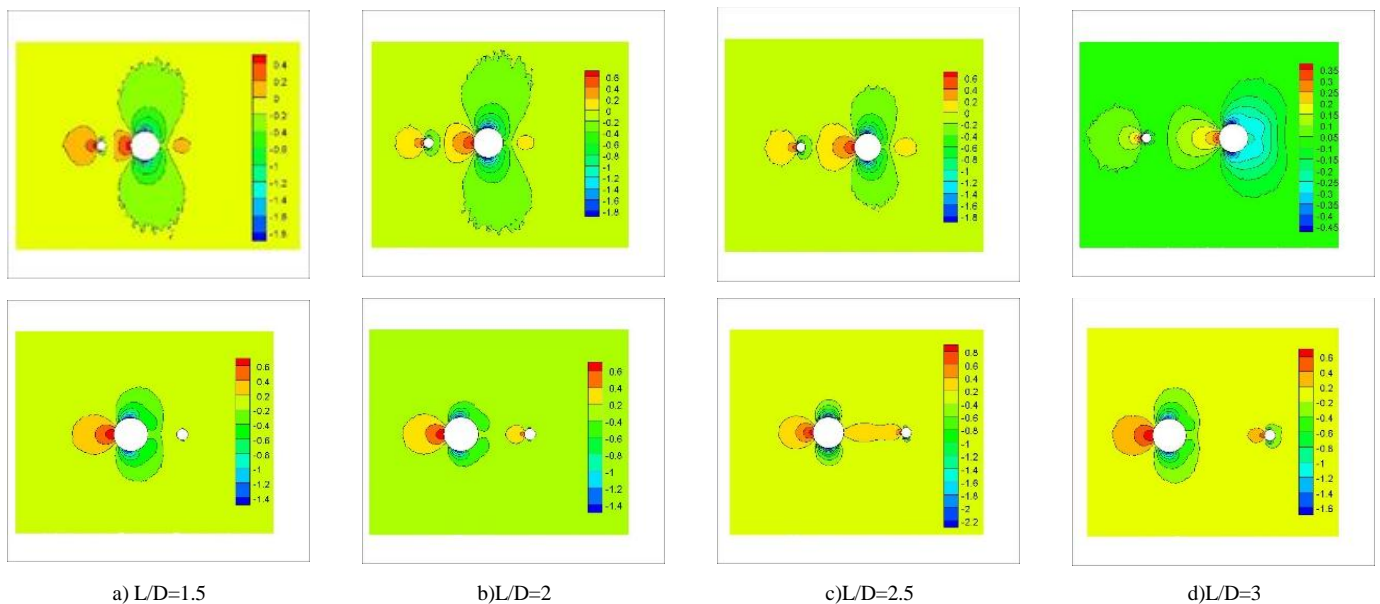


Figure 4. Cp contours of STA and TSA for different L/D with k-ε model

Figures (5 and 6a,b and c) show the streamlines pattern and velocity vectors for the TSA and STA at plane Z/H=0.05, and L/D=1.5, 2 and 3. From figures it is obvious that the vortex structures in TSA (in gap between buildings) are more regular than those observed in STA and the plane boundaries have a

modulation effect on the flow. In both TSA and STA, when the building spacing is increased to a threshold the wake structure translates from the reattachment regime to the co-shedding regime. Also in STA there is no flow interaction in the gap between cylinders and the shear layers emerging from

upstream cylinder side form vortices at downstream cylinder. Figure (7) shows the variation of  $C_p$  with angle  $\theta$  of the upstream building for both TSA and STA at  $Z/H=0.05$  and different  $L/D$ . It is shown that  $C_p$  values variation is approximately constant for all  $L/D$  values from  $\theta=0^\circ$  till  $\theta=45^\circ$ , then as  $\theta$  increases to  $90^\circ$   $C_p$  decreases to get its

lowest value at  $L/D=2$  and maximum value at  $L/D=2.5$ , also  $C_p$  is almost constant in values for both  $L/D=3$  and  $1.5$  in TSA and STA respectively in the range of  $90^\circ \leq \theta \leq 270^\circ$ . Figure (8) shows the variation of  $C_d$  with diameter ratios ( $B$ ), it is shown that as the diameter ratio increases the drag coefficient increases for both arrangements.

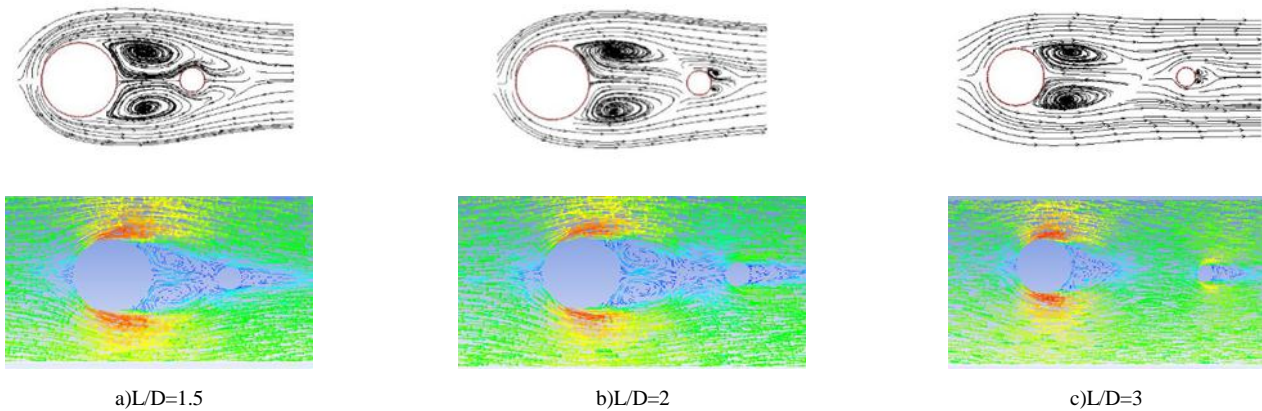


Figure 5. Streamlines pattern and velocity vectors for TSA and different  $L/D$  with  $k-\epsilon$  model

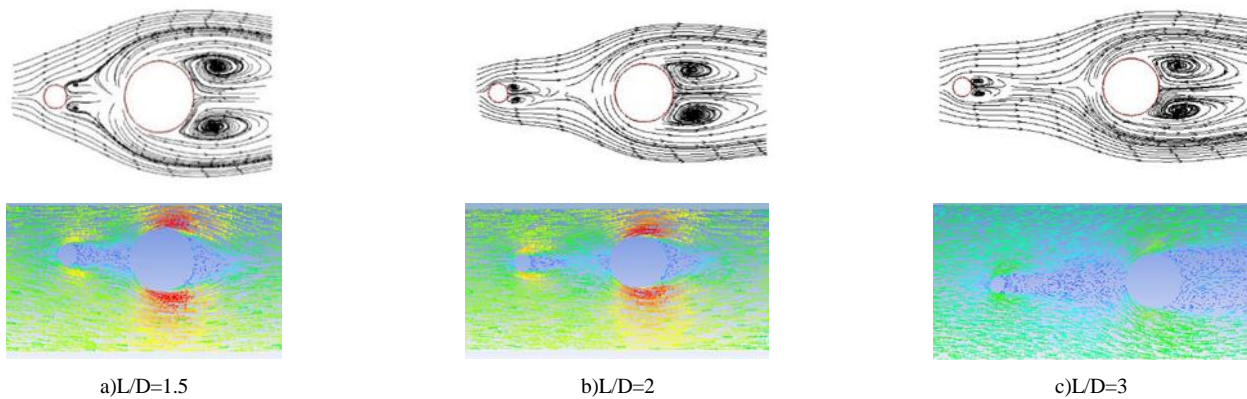


Figure 6. Streamlines pattern and velocity vectors for STA and different  $L/D$  with  $k-\epsilon$  model

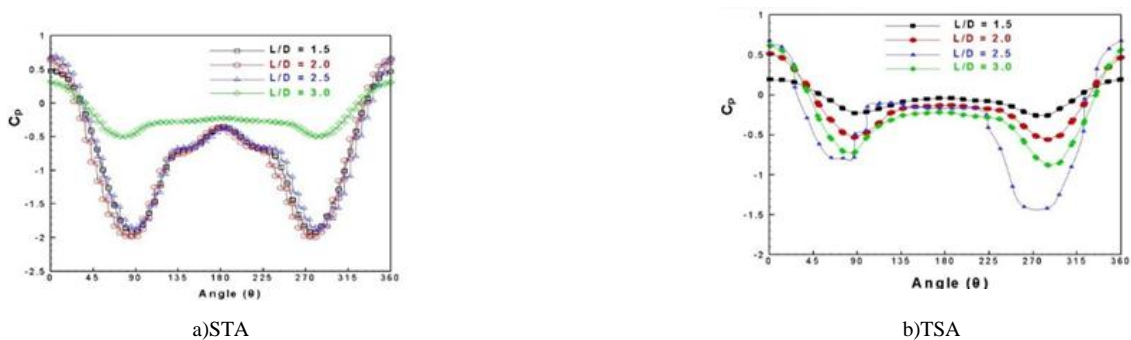


Figure 7.  $C_p$  distribution of upstream building for different  $L/D$  at  $Z/H=0.05$  with  $k-\epsilon$  model.

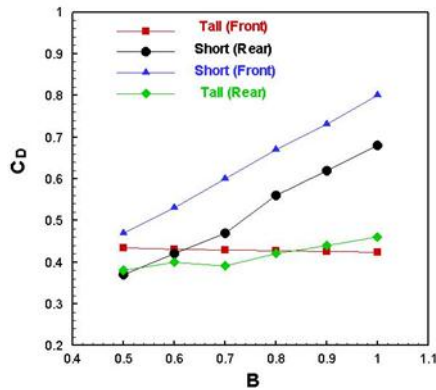


Figure 8. Distribution of Cd with the diameter ratio (B) for the upstream and downstream buildings with k-ε model

### C. k-ε (RNG) Results

Figures (9 a,b,c and d) show Cp contours of STA and TSA for different gaps ( $L/D=1.5, 2, 2.5$  and  $3$ ) at plane ( $Z/H=0.05$ ). It is obvious in figures for both STA and TSA that the center-to-center separation ( $L/D$ ) effect the Cp contours distribution in the flow around buildings, also the stagnation point at the front building is clear but it is not clear at the rear one in TSA, this is because the rear building lies in the wake region of the front tall building but in STA the two stagnation points are clear for the two buildings. For all  $L/D$  values, a pair of almost symmetrical vortices is formed in the gap between the buildings. If the gap is gradually increased to  $L/D=3$  as shown in figures the shedding regime eventually changes to alternating in gap in which regions of concentrated vortices grow and decrease alternatively on each side of the line that links the centers of the buildings.

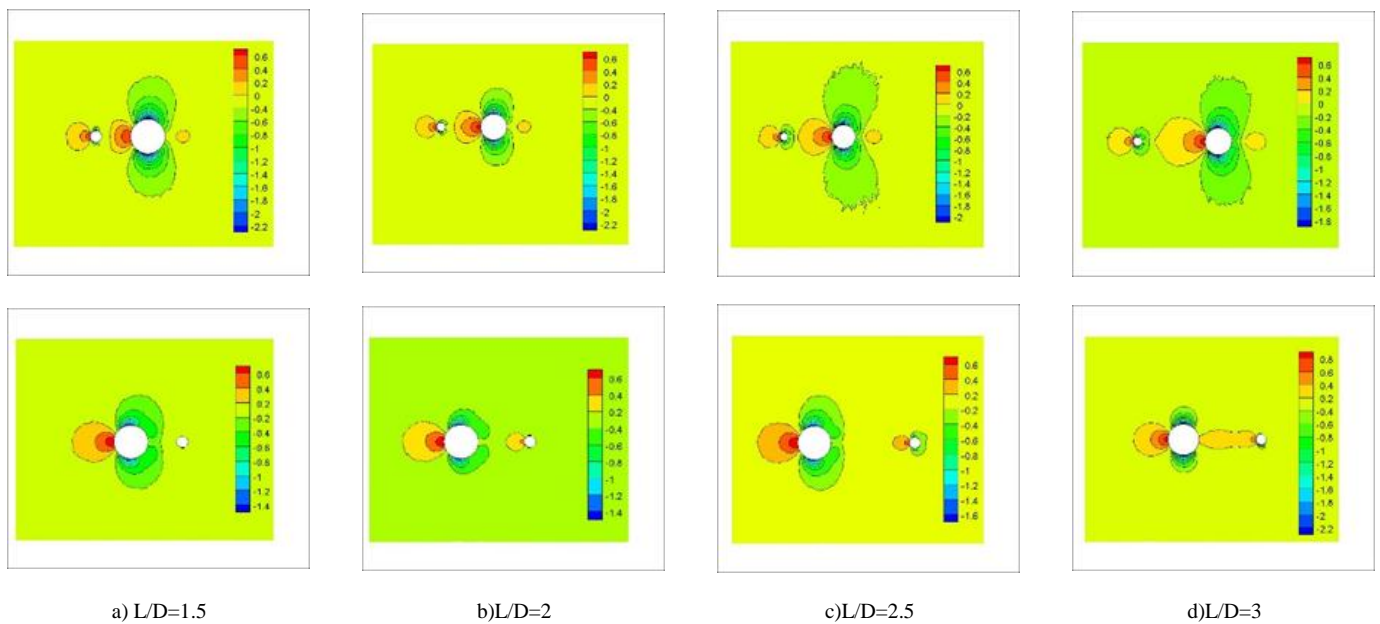


Figure 9. Cp contours of STA and TSA for different  $L/D$  with k-ε (RNG) model

Figures (10 and 11) show the streamlines pattern and velocity vectors for the TSA and STA at plane  $Z/H=0.05$ , and  $L/D=1.5, 2$  and  $3$ . From figures it is obvious that the vortex structures in TSA and STA are formed. In both TSA and STA, downstream of buildings a Karmen Vortex Street seems to be formed due to alternate generation of vortices, also the streamlines and velocity vectors confirm the alternate generation of vortices within the gaps and also at downstream positions, as in Zdravkovich [13]. Also in STA there is no flow

interaction in the gap between buildings and the shear layers emerging from upstream building side form vortices at downstream building. Figure (12) show the variation of Cp with angle  $\theta$  for the upstream tall building at  $Z/H=0.05$  and different  $L/D$ . It is shown that Cp values in STA has its min. value at  $\theta=90^\circ$  and max. value at  $\theta=180^\circ$  for all  $L/D$  values, then as  $\theta$  increases to  $360^\circ$  Cp behaves in a similar way as in range of  $0 \leq \theta \leq 180$ .

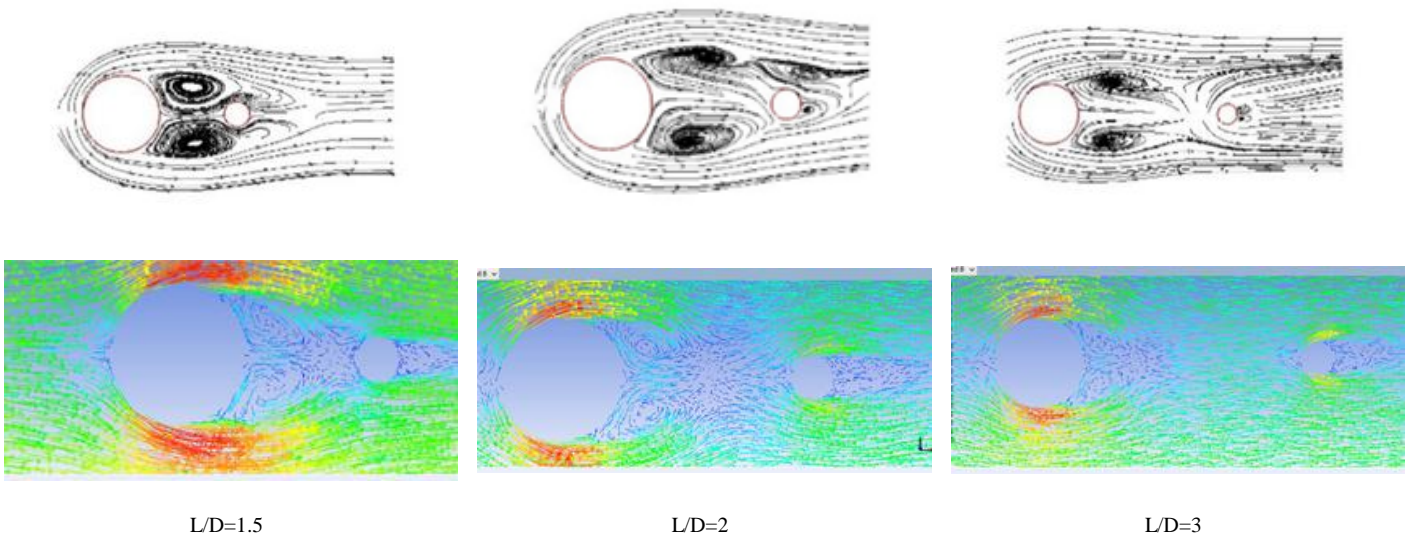


Figure 10. Streamlines pattern and velocity vectors for TSA and different L/D with k-ε (RNG) model

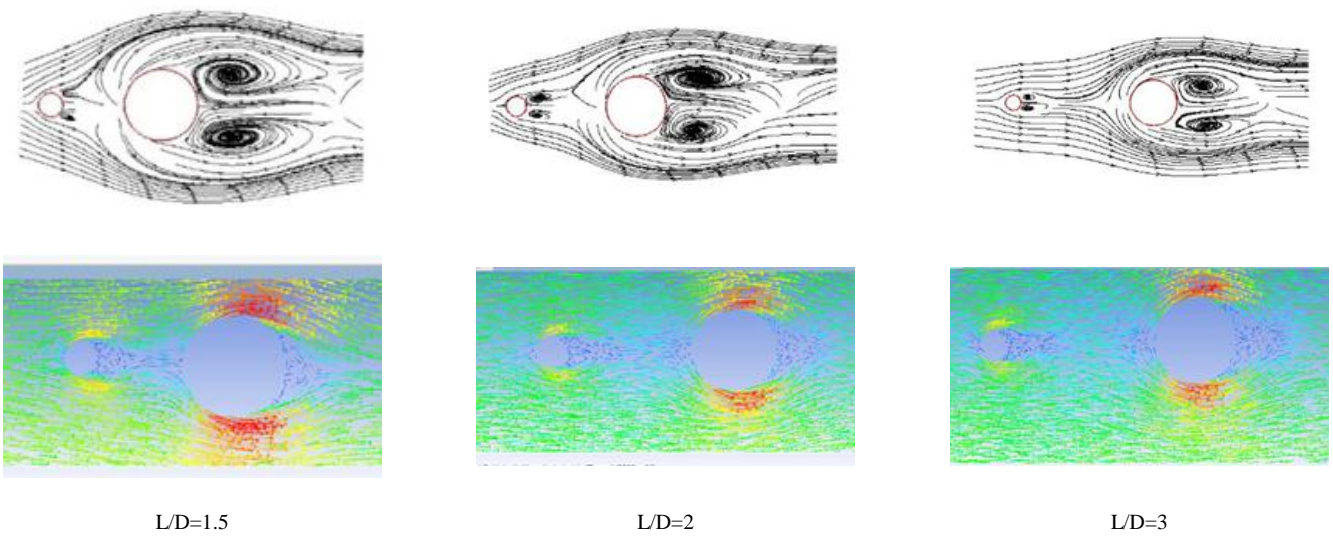


Figure 11. Streamlines pattern and velocity vectors for STA and different L/D with k-ε (RNG) model

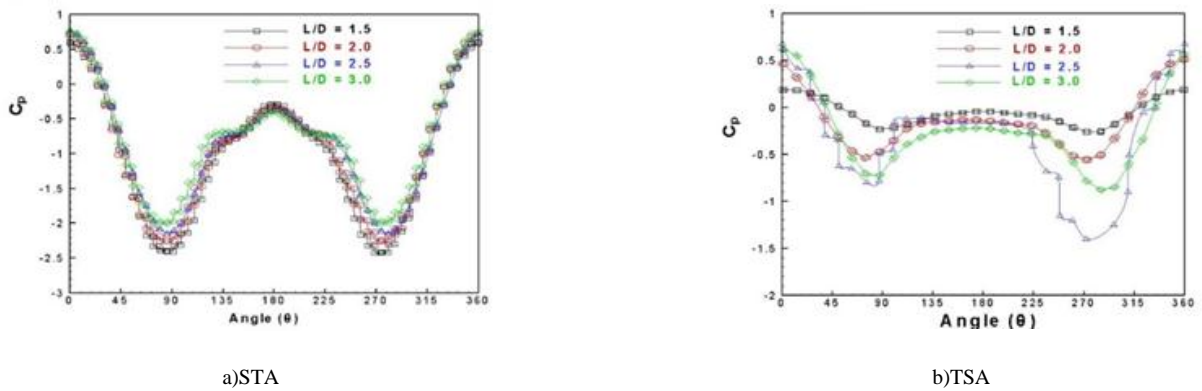


Figure 12. Cp distribution of upstream building for different L/D at Z/H=0.05 with k-ε (RNG) model.

Figure 13 shows the graph of Strohal number  $St$  and  $Re$ , according to the relation between  $St$ ,  $Re$  and the vortex shedding frequency we note from graph that as  $Re$  increases  $St$  increases for both tall and short buildings. That is as the flow velocity increases the vortex shedding increases behind the building either for tall or short building.

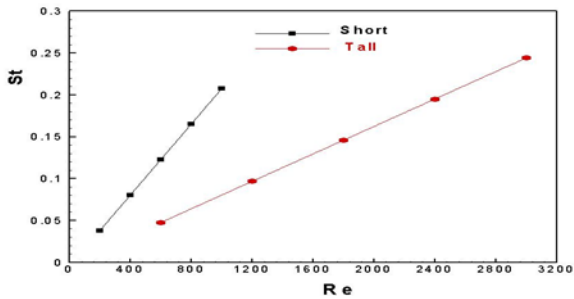


Figure 13.  $St$  Distribution with  $Re$  for both short and tall buildings

#### D. LES Results

Figures (14 a, b, c and d) show  $C_p$  contours of STA and TSA for different gaps ( $L/D=1.5, 2, 2.5$  and  $3$ ) at plane ( $Z/H=0.05$ ). It is clear for both STA and TSA that there is an irregularity in  $C_p$  contours distribution around buildings, also the center-to-center separation ( $L/D$ ) affect the flow regime. The stagnation point at the front building is clear but it is not clear at the rear one in TSA, this is because the rear building lies in the wake region of the front tall building but in STA the two stagnation points are clear for the two buildings. In this regime, a pair of almost unsymmetrical vortices is formed in the gap between the buildings. If the gap is gradually increased to  $L/D=3$  as shown in figures the shedding regime eventually changes in an irregular way.

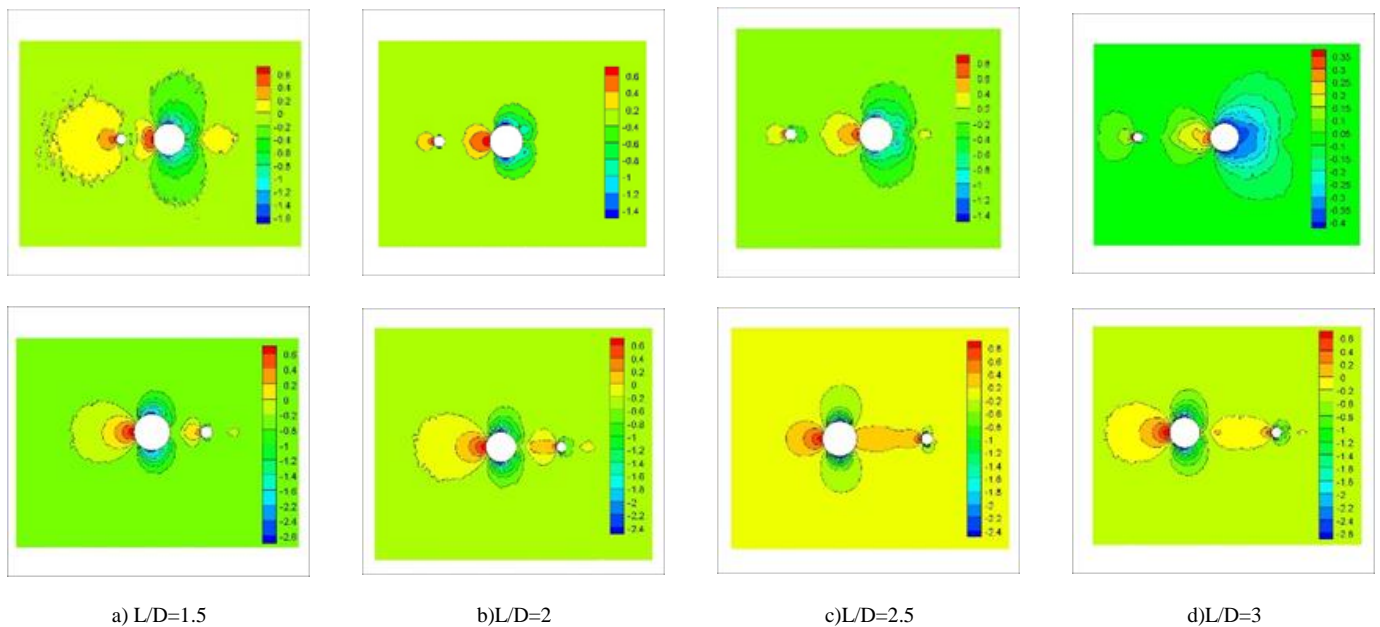


Figure 14.  $C_p$  contours of STA and TSA for different  $L/D$  with LES model

Figures (15 and 16) show the streamlines pattern and velocity vectors for the TSA and STA at plane  $Z/H=0.05$ , and  $L/D=1.5, 2$  and  $3$ . From figures it is obvious that the vortex structures in TSA and STA are irregular. Also in STA there is no flow interaction in the gap between buildings and the shear layers emerging from upstream building side form vortices at

downstream building. Figure (17) shows the variation of  $C_p$  with angle  $\theta$  for the upstream tall building at  $Z/H=0.05$  and different  $L/D$ . It is shown that there is a singular distribution for  $C_p$  values at  $L/D=3$  for STA and the max. and min. values of  $C_p$  at  $\theta=180^\circ$  and  $\theta=90^\circ$  respectively, then as  $\theta$  increases the curve repeats itself.

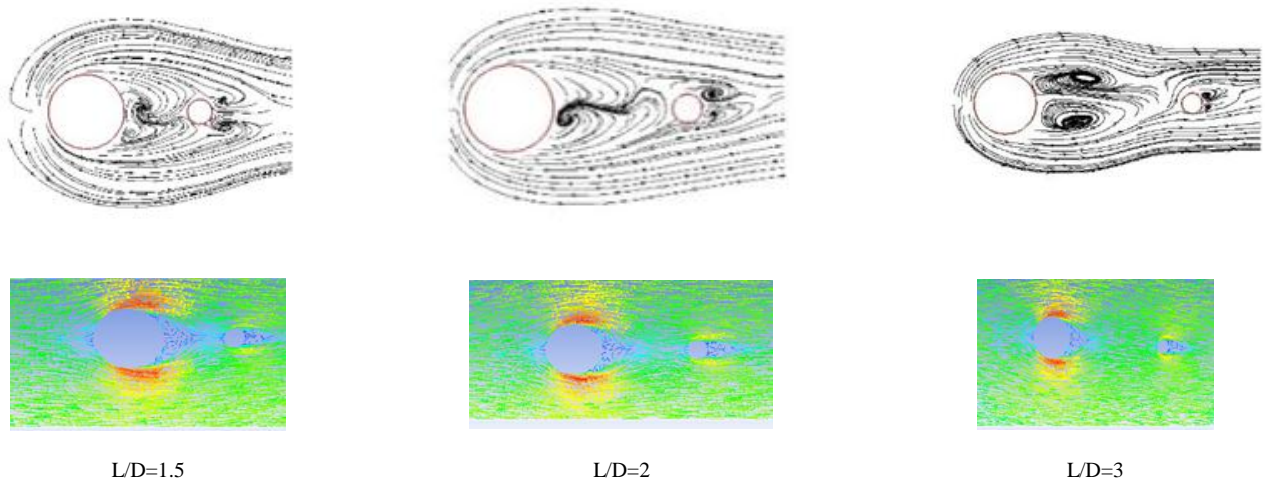


Figure 15. Streamlines pattern and velocity vectors for TSA and different L/D with LES model

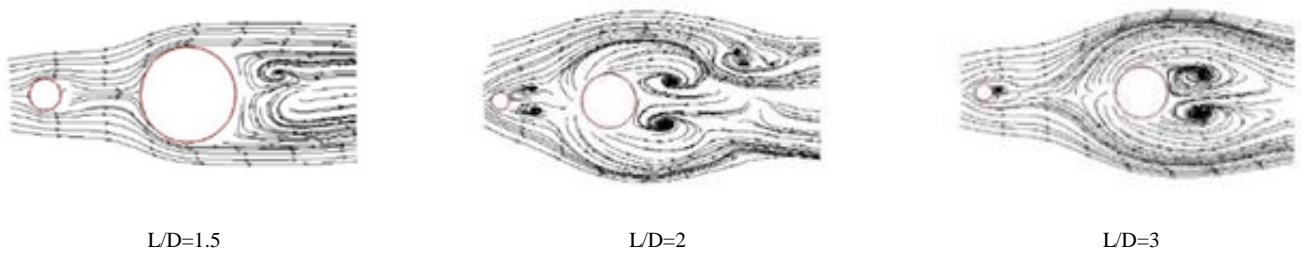
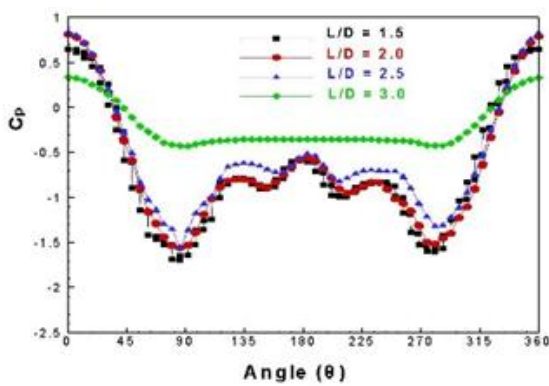
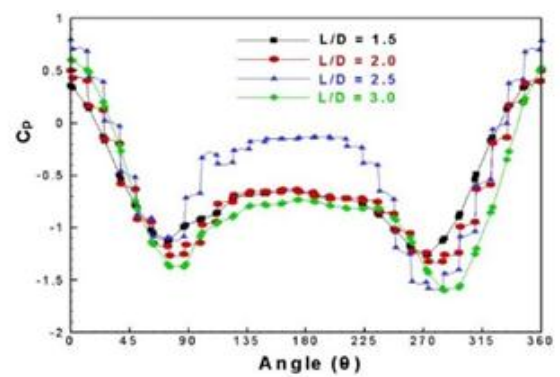


Figure 16. Streamlines pattern for STA and different L/D with LES model



a)STA



b)TSA

Figure 17. Cp distribution for upstream building for different L/D at Z/H=0.05 with LES model



At end of this discussion we note that for all turbulent models at  $L/D=2.5$ , the vortices are not fully developed due to an abrupt changes in flow characteristics, so the drag force acts as thrust force due to the pressure difference between rear and front side of the downstream building, so we can consider this space as a critical one.

#### E. Comparison Between $k-\epsilon$ , $k-\epsilon(RNG)$ and LES Results

Figure (18a, b and c) shows the contours of  $C_p$  along the buildings in TSA and STA for different turbulent models, it is clear from the comparison that  $k-\epsilon$  (RNG) model is the most regular reasonable one than the other turbulent models.

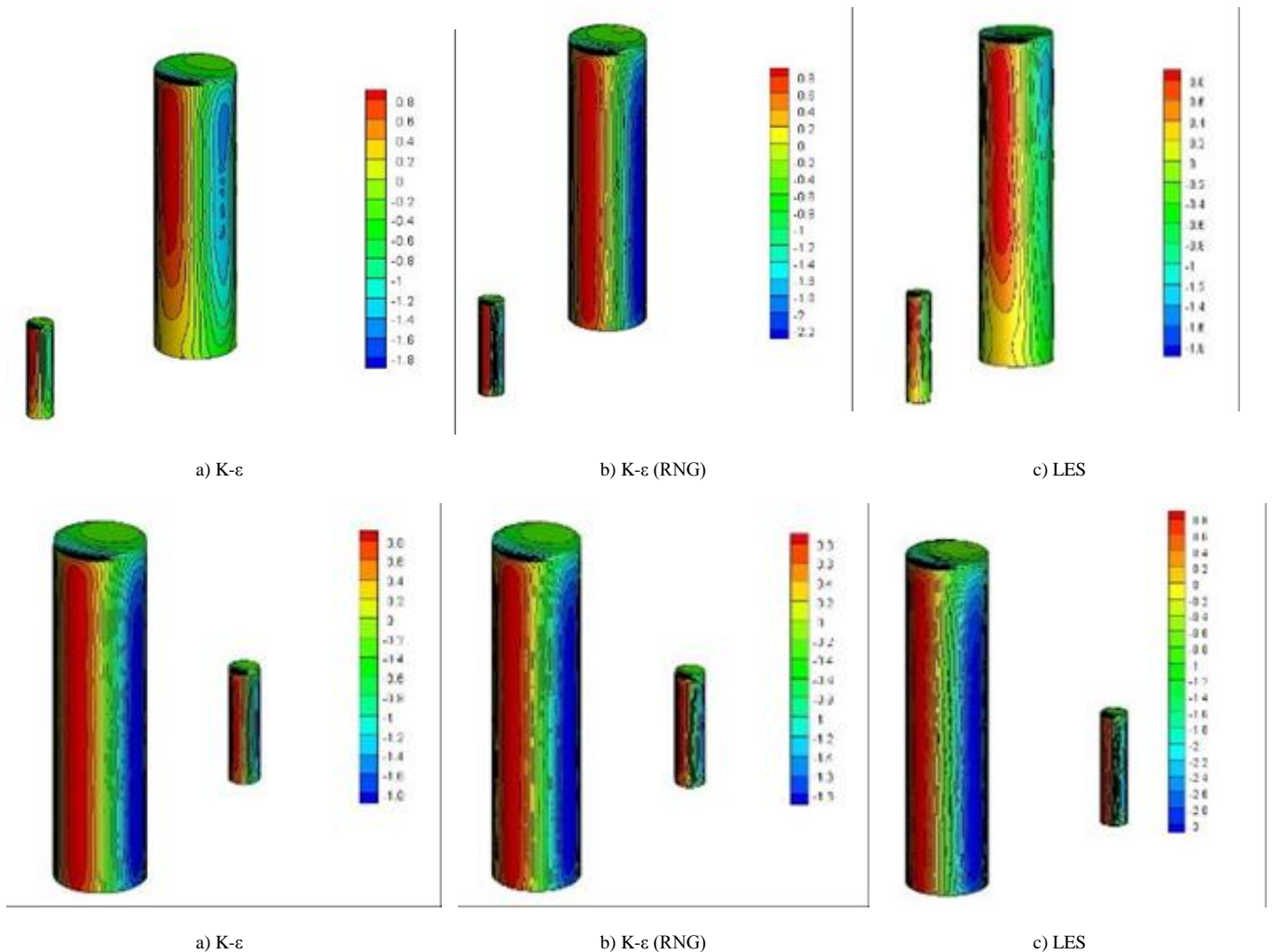


Figure 18. A comparison between different turbulent models of  $C_p$  contours for both TSA and STA for  $L/D=3$  at  $Z/h=0.05$

Figure 19 shows a comparison between the turbulent models for the distribution of  $C_D$  with variation of  $L/D$  for both upstream tall and short buildings at  $Z/H=0.05$ . It is clear from figure that values of  $C_D$  (for tall buildings for the three turbulent models) increases as  $L/D$  increases and at  $L/D=2$   $C_D$  has the same value, also  $k-\epsilon$  (RNG) model has the least values of  $C_D$  for both short and tall buildings. Also for upstream short buildings,  $C_D$  values are more higher than for tall buildings

and there is no variation in  $C_D$  with the variation of  $L/D$  especially in  $k-\epsilon$  (RNG) model and also according to Yakhot [14],  $k-\epsilon$  (RNG) ,the turbulent model used in numerical solution, has shown an excellent agreement between numerical and experimental results for an isothermal flow over backward facing step, therefore for these reasons,  $k-\epsilon$  (RNG) is more suitable for these applications and the LES turbulent model is the worst one for these applications.

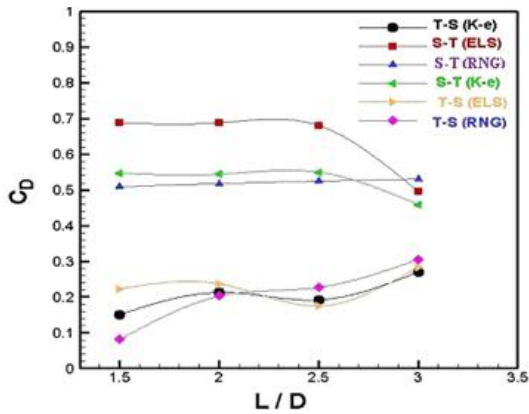


Figure 19. Comparison between different turbulent models for CD with L/D at Z/H=0.05 for upstream tall and short buildings

#### IV. UNCERTAINTY ANALYSIS

According to P.J. Roache, (1997), the errors in a fine and coarse grids (E1fine, E2coarse) and grid convergence index (GCI) are given by:

$$E1_{fine} = (f2-f1) / (1-rp) \text{ and } E2_{coarse} = rp \times E1_{fine}$$

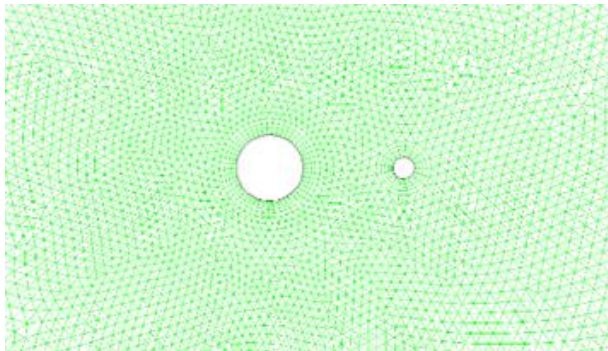
$$GCI1_{fine} = FS \times (abs E1_{fine}) \text{ and } GCI2_{coarse} = FS \times (abs E2_{coarse})$$

From the data of both fine and coarse grids ( $r=5/3$  and  $p=0.99$ ) and according to the numerical solution, let  $f1$  and  $f2$  be the stagnation pressure and  $FS=3$ . Table (3) shows the errors and grid convergence index values.

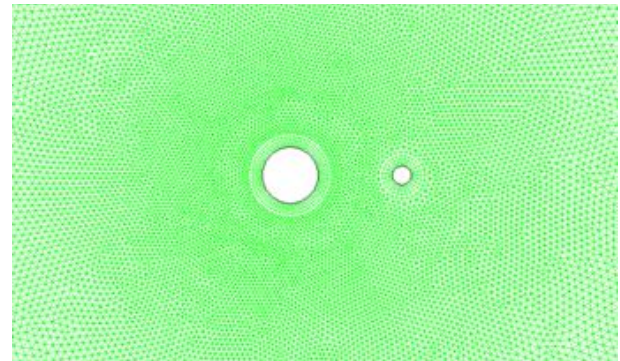
In addition to this table, Fig. 20 represents the fine and coarse grids at the mid height plane and part of results of residuals for both fine and coarse grids.

TABLE I. ERRORS AND GRID CONVERGENCE INDEX VALUES

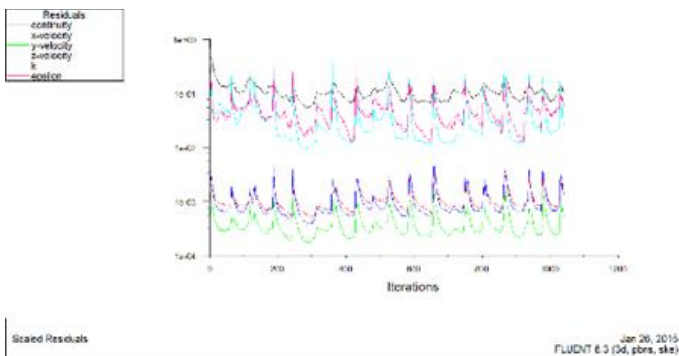
Number of fine grid points	Number of coarse grid points	$P_{fine}$ , pa	$P_{coarse}$ , pa	$E1_{fine}$	$E2_{coarse}$	$GCI1_{fine}$	$GCI2_{fine}$
500000	300000	49.887	49.945	0.03817	0.06046	0.11451	0.18137



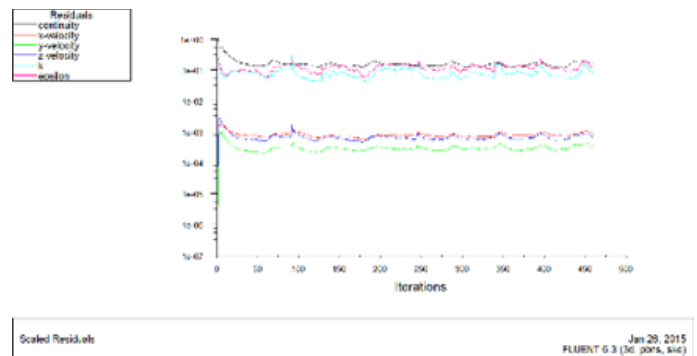
a) Coarse mesh



b) Fine mesh



a. Coarse mesh residuals



b. Fine mesh residuals

Figure 20. Part of residuals and grids of the numerical solution

## V. CONCLUSIONS

A thorough investigation of the possible flow patterns around two circular buildings (TSA and STA) in tandem arrangements at  $1000 \leq Re \leq 3000$ ,  $L/D=1.5, 2, 2.5$  and 3 and diameter ratios  $0.5 \leq B \leq 3$  was presented. Based on the above discussions, we can conclude that the discussions show good agreements between the experimental and numerical results and the presence of three-dimensional flow structures was observed to induce notable changes in  $C_p$  to the variation of building gap. It is observed that the gap between the two buildings affects the flow regime, i.e., there is a distinct vortex shedding downstream of the first building. Also for the flow past two buildings, the average value of  $C_p$  of the front tall building is approximately 2.3 times the value for that of the downstream short building. Also, the lowest value of  $C_p$  for two buildings is at angle  $\theta=90^\circ$ . Since the drag force decreases on the rear low height building because of the effect of wakes, therefore we can use this result in reducing the quantity of materials used in structure of the rear building and so the cost of its structure can reach to approximately 0.4 of the structure cost of the front building, also the positive drag coefficient in STA increases as the diameter ratio increases and  $k-\epsilon$  (RNG) is more suitable for these applications but ELS is not suitable for these applications. The Strouhal number and so the vortex shedding frequency behind the buildings increases as  $Re$  increases. The gap  $L/D=2.5$  is found to be critical for all turbulent models due to abrupt changes in flow characteristics. For STA  $C_D$  is approximately constant for all turbulent models but its value is the least one for  $k-\epsilon$  (RNG). Finally the uncertainty for the numerical results shows that the errors are acceptable, also the analysis presented helps to improve the understanding of flows with wake interference, and can be very useful for future investigations of other aspects of such flows.

## VI. ACKNOWLEDGMENT

The author would like to thank Prof. Dr. N.M. Guirguis and Eng. Wael for their valuable discussions towards the paper materials.

## REFERENCES

[1] Mof.M.N.,2014,“Experimental and Numerical Study of Three Dim. Unsteady Incompressible Flow past Two Identical Circular Cylinders in Tandem Arrangements” JMEA, USA Vol.4 No. 5.  
 [2] Zaheer I. , S. Ahmad, M. Muzzammil, 2011, “ Numerical Predication of Wind Loads on Low Buildings.” International Journal of Engineering Science and Technology,Vol.3,No.5,pp: 59-72.

[3] A. Sohankar. 2012, “A Numerical Investigation of the Flow Over a Pair of Identical Square Cylinders in a Tandem Arrangement.” I. J. for Num. Methods in Fluids. Vol.70,pp: 1244-1257.  
 [4] I.Ehsan and S. Mohmmad, 2013,“Power Law Fluid Flow Passing Two Square Cylinders in Tandem Arrangement”. J. of Fluids Eng.,Vol.135, 8pages.  
 [5] Y.Kada and F. Sanglun,2013,“Aerodynamics Effects of the Early Three-Dim. Instabilities in the Flow Over One and Two Circular Cylinders in Tandem Predicated by the Lattice Boltzman Method”. J. of Comp. and Fluids, Vol.74, pp.32-43.  
 [6] Y. Gao and X.Yang,2013,“Particle Image Velocimetry Technique Measurements Near Wake Behind a Cylinder- Pair of Unequal Diameters”. J. of Fluid Dyn., Vol.45.  
 [7] Kopp G., 2014, “Wind Loads on Low- Profile, Tilted, Solar Arrays Placed on Large, Flat Low- Rise Building Roofs.” Journal of Structural Engineering, Vol. 140 Issue 2.  
 [8] Renjie Jiang, Jianzhong Lin and Xiaokeku, 2014, “Numerical predications of Flows Past 2 Tandem Cylinders of Different Diameters Under Unconfined and Confined Flows.” J of Fluid Dynamic Research, Vol.46, No.2.  
 [9] Ming Ming Liu, Lin Lu, and Bin Teng, 2014, “Re- Examination of Laminar Flow Over Twin Circular Cylinders in Tandem Arrangement.” J of Fluid Dynamic Research, Vol.46, No.2.  
 [10] S.K.Verma, 2014, “Wind Loads on Structurally Coupled Through Single Bridge Tall Buildings.” IJournal of Civil and Structural Engineering, Vol.4, No.3.  
 [11] Micheal Jesson, Mark Sterling, Chris Letchford and Matthew Haines,2015, “Aerodynamic Forces on Generic Buildings Subject to Transient Downburst-Type Winds.” Journal of Wind Engineering and Industrial aerodynamics, Vol.137,pp:58-68.  
 [12] K.R.Sreenivasan, P.J.Strykowski and D.J. Olinger, “Hopf Bifurcation Landau Equation and Vortex Shedding Behind Circular Cylinder.” Department of Mech. Eng. And Center for Applied Mechanics, Yale University, New Haven Connecticut.  
 [13] M. M.Zdravkovich,1987, “The Effect of Interference Between Circular Cylinders in Cross Flow.” Journal of Fluid Structures,pp.239-261.  
 [14] Yakhot V, Orszag SA, Thangam S, Gatski TB, Speziale GG, 1992, “ Development of Turbulence Models for Shear Flows by a Double Expansion Technique”. J.Phys Fluids A 4, 1510–1520.  
 [15] ANYSES, 15.0.7,CFD, Program.  
 [16] P.J. Roache ,1997, “Quantification of Uncertainty in Computational Fluid Dynamics.” J. of annu. Rev. Fluid Mech.,Vol.29, pp.123-160.



**Mofreh Melad Nassief** is currently an associated professor in Power Mechanical Engineering Department, Zagazig University, Egypt. He received his PhD in 1995. His research interests include fluid structure interaction, and heat and mass transfer.